Title

Ganglion Cell Complex: The Optimal Measure for Detection of Structural Progression in the Macula.

Authors

Mohammadzadeh, Vahid
Su, Erica
Rabiolo, Alessandro
et al.

Publication Date

2022-05-01

DOI

10.1016/j.ajo.2021.12.009

Peer reviewed

HHS Public Access

Author manuscript

Am J Ophthalmol. Author manuscript; available in PMC 2023 May 01.

Published in final edited form as:

Am J Ophthalmol. 2022 May ; 237: 71–82. doi:10.1016/j.ajo.2021.12.009.

Ganglion Cell Complex: The Optimal Measure for Detection of Structural Progression in the Macula

Vahid Mohammadzadeh, MD[1], **Erica Su, MS**[2], **Alessandro Rabiolo, MD, FEBO**[3], **Lynn Shi, MD**[1], **Sepideh Heydar Zadeh, MS**[1], **Simon K. Law, MD, PharmD**[1], **Anne L. Coleman, MD, PhD**[1], **Joseph Caprioli, MD**[1], **Robert E. Weiss, PhD**[2], **Kouros Nouri-Mahdavi, MD, MS**[1]

[1]Glaucoma Division, Stein Eye Institute, David Geffen School of Medicine, University of California Los Angeles, Los Angeles, California

[2]Department of Biostatistics, Fielding School of Public Health, University of California Los Angeles, Los Angeles, California

[3]Department of Ophthalmology, Gloucestershire Hospitals NHS Foundation Trust, Cheltenham, UK

Abstract

Purpose.—Test the hypothesis that macular ganglion cell complex (GCC) thickness from optical coherence tomography (OCT) provides a stronger change signal regardless of glaucoma severity compared to other macular measures.

Design: Prospective cohort study.

Setting: Tertiary glaucoma center.

Subjects: 112 eyes with moderate to severe glaucoma at baseline.

Observation Procedure: In each 3°×3° macular superpixel, a hierarchical Bayesian random intercept and slope model with random residual variance was fit to longitudinal full macular thickness (FMT), outer retina layers (ORL), GCC, ganglion cell/inner plexiform layer (GCIPL),

Corresponding author: Kouros Nouri-Mahdavi, MD, MS, 100 Stein Plaza, Los Angeles, CA, 90095, USA, Phone: 310-794-1487, Fax: 310-794-6616, nouri-mahdavi@jsei.ucla.edu.

Presented as a paper at the American Glaucoma Society annual meeting, March 4, 2021.

CRediT author statement

Mohammadzadeh, Vahid; Methodology, Software, Investigation, Resources, Formal Analysis, Writing - Original Draft, Visualization **Su, Erica;** Methodology, Software, Investigation, Formal Analysis, Writing - Original Draft, Visualization, Data Curation **Rabiolo, Alessandro;** Writing - Review & Editing **Shi, Lynn;** Data collection **Heydar Zadeh, Sepideh;** Data collection **Law, Simon K.** Writing - Review & Editing, Validation **Coleman, Anne L.** Writing - Review & Editing, Validation **Caprioli, Joseph;** Writing - Review & Editing, Validation **Weiss, Robert E.;** Methodology, Software, Supervision, Project administration, Formal Analysis, Writing - Original Draft, Funding acquisition. **Nouri-Mahdavi, Kouros;** Conceptualization, Methodology, Resources, Investigation, Validation, Formal Analysis, Data Curation, Writing - Original Draft, Visualization, Supervision, Project administration, Funding acquisition

and ganglion cell layer (GCL) measurements. We estimated population- and individual-level slopes and intercepts.

Main outcome measures: Proportions of significant worsening and improving superpixel slopes were compared between layers and in superpixels with mild/moderate vs. severe damage (total deviation of corresponding visual field location ≥−8 vs. <−8dB).

Results.—Average (SD) follow-up time and baseline 10-2 visual field mean deviation were 3.6 (0.4) years and −8.9 (5.9) dB. FMT (54.9%) displayed the highest proportion of significant negative slopes followed by GCC (36.5%), ORL (35.6%), GCIPL (30.6%), and GCL (19.8%). Inner macular measures detected less worsening in the severe glaucoma group; yet GCC (22.6%) identified the highest proportion (GCIPL:18.6%; GCL:10.8%). Proportions of positive rates were small and comparable among all measures.

Conclusions.—GCC is the optimal macular measure for detection of structural change in eyes with moderate to severe glaucoma. Although a higher proportion of worsening superpixels was observed for FMT, a large portion of FMT change could be attributed to changes in ORL.

Graphical Abstract

We provide strong evidence that ganglion cell complex (GCC) thickness may be the optimal macular outcome measure for detection of glaucoma progression in moderately severe to advanced stages of the disease. We recommend macular GCC thickness measurements be made available on all OCT devices for optimizing detection of glaucoma progression.

Keywords

Optical Coherence Tomography; macula; progression; ganglion cell complex; ganglion cell/inner plexiform layer; ganglion cell layer; full macular thickness; outer retinal layers; ORL; longitudinal; Bayesian; hierarchical model

Introduction

Macular optical coherence tomography (OCT) is now considered the standard imaging modality for assessing central retinal ganglion cells (RGC). [1–4] Macular damage can be detected in a large proportion of patients with early perimetric glaucoma. [5–8] Macular RGCs are among the last remaining cells in advanced glaucoma. Therefore, macular OCT imaging may be able to detect changes in the RGCs and related components across the spectrum of glaucoma severity. [2,7,9–11] Timely detection of glaucoma progression, especially in the central macula, is crucial for prevention of irreversible and visually disabling functional impairment. There is evidence that glaucomatous structural progression in the macula can be detected earlier than functional (visual field) changes in some patients. [5,12–14] Various OCT devices provide different macular structural outcome measures ranging from full macular thickness (FMT) to ganglion cell complex (GCC), ganglion cell/inner plexiform layer (GCIPL), or ganglion cell layer (GCL) thickness measurements. While there is no evidence that any of the inner macular outcome measures is superior for detection of early glaucoma, there are reasons to believe that they may perform differently for detection of structural glaucoma progression. As glaucoma progresses, the tissue density and density

gradients between consecutive layers of the retina may change and hence segmentation of the individual retinal layers becomes more challenging and noisier for the automated algorithms of the OCT devices. We hypothesized that GCC thickness would perform best for detection of glaucoma deterioration especially in the more advanced stages of glaucoma as disease worsening leads to progressive thinning of the macula and segmentation of individual retinal layers becomes more challenging.

Rabiolo and collaborators recently compared rates of structural change at the level of superpixels for full macular thickness (FMT), ganglion cell complex (GCC), ganglion cell/inner plexiform layer (GCIPL), ganglion cell layer (GCL) and outer retina layers (ORL) in a cohort of eyes with moderate to advanced glaucoma damage at baseline. [15] The FMT and GCC thickness, in that order, displayed the fastest rates of progression; however, a significant proportion of FMT changes could be explained by thinning of the ORL, which is not characteristic of glaucoma deterioration. [16–18] Therefore, GCC was proposed as potentially the optimal outcome measure for detecting glaucoma progression in the macula. In another study, Mohammadzadeh et al. found that GCC rates of change showed the highest longitudinal structure-function (SF) correlation with central visual field (VF) slopes. [13]

Both Rabiolo et al. and Mohammadzadeh and colleagues used univariate regressions of thickness measurements at the superpixel or sectoral level. Univariate regression analyses applied to numerous longitudinal macular superpixel measurements have shortcomings: population-level information contained within the study cohort is not used to estimate individual rates of change; correlations between repeated measurements on subjects are not incorporated into the analysis. Longitudinal data analysis using random effects models are able to model all subjects' data over time and can incorporate population information and correlations over time and therefore, more accurately estimate structural rates of change. [19–28] We recently proposed a hierarchical Bayesian model with random intercepts and slopes to estimate subject- and population-level rates of change within macular superpixels. [29] Use of random effects allows modeling subject-specific effects more efficiently and accurately and allows population information to help estimate individual trends; it also enables estimation of subject-specific mean and trend variances and their correlation correctly.

The aim of this study is to test the hypothesis that GCC thickness is the optimal macular measure for detecting structural change in the macula in eyes with moderate to severe glaucoma within our recently developed Bayesian hierarchical framework. Main outcome measures were the proportions of significant negative and positive rates of changes in each superpixel and separately according to the level of glaucoma damage in the superpixel.

Methods

Study sample

We analyzed data from 112 eyes (112 subjects) from the Advanced Glaucoma Progression Study (AGPS), an ongoing, prospective, longitudinal study at the University of California Los Angeles. The Institutional Review Board (IRB) approved this study and the study adhered to the tenets of the Declaration of Helsinki and the Health Insurance Portability and

Accountability Act (HIPAA) policies. All patients provided written informed consent at the time of enrollment in the study.

The enrolled eyes met the following inclusion criteria: a) clinical diagnosis of primary open-angle glaucoma, pseudoexfoliative glaucoma, pigmentary glaucoma, or primary angle-closure glaucoma; b) evidence of either central damage on 24-2 VF, defined as two or more points within the central 10° with $p < 0.05$ on the pattern deviation plot or VF mean deviation (MD) worse than −6 dB. Exclusion criteria were baseline age less than 39 years or greater than 80 years; best-corrected visual acuity worse than 20/50; refractive error exceeding 8 diopters (D) of sphere or 3 D of cylinder; any significant retinal or neurological disease potentially affecting OCT measurements. Study eyes had no other ocular pathology at baseline and underwent clinical exams, imaging and visual field testing approximately every 6 months. We analyzed observations up to 4.25 years after baseline. Data from visits less than 0.2 years after a previous visit were omitted. [29]

Macular OCT imaging

The Spectralis spectral-domain OCT (Heidelberg Engineering, Heidelberg, Germany) was used to obtain macular volume scans. The Posterior Pole Algorithm of the Spectralis OCT acquires 30°×25° volume scans of the macula (61 B-scans spaced approximately 120 μm apart) centered on the fovea. Each B-scan was repeated 9-11 times to reduce speckle noise. Proprietary software of Spectralis OCT, the Glaucoma Module Premium Edition software, was used to automatically segment individual retinal layers before data export. Images were reviewed for segmentation errors and image artifacts. Any obvious segmentation errors were manually corrected with the SD-OCT device's built-in software. If more than two B-scans within the central 24° of any individual volume scans were of inadequate quality or showed poor segmentation, that session was excluded from analyses. A low-quality B-scan image was defined as quality factor <15, presence of more than 10% missing data or inadequate segmentation, or any artifacts such as mirror artifacts. After segmentation, the individual layer thickness measurements are provided as 8×8 arrays of 3°×3° superpixels for the central 24°×24° region centered on the fovea.

The retinal nerve fiber layer (RNFL), GCL, and inner plexiform layer (IPL) thickness measurements were summed to calculate the ganglion cell complex (GCC) measurements, representing tissue delimited by the internal limiting membrane and the IPL/inner nuclear layer (INL) boundary; GCIPL thickness measurements were calculated by adding the GCL and IPL layers; this represents the thickness of an area delimited by the RNFL/GCL boundary and the IPL/INL boundary.

Due to the substantial measurement noise in peripheral macular regions, we only included the central 36 (6×6 or 18°×18°) superpixels for further analyses (Figure 1). [30] This approximately matches the area imaged and analyzed by Cirrus high-definition OCT.

Data inspection, exploration and outlier removal for each macular layer

Our methods have been previously described in detail; [29] identical procedures were used here for all layers. Briefly, for each superpixel and macular outcome, including FMT, ORL, GCC, GCIPL, and GCL thickness, we plotted data in profile plots and empirical summary

plots. [29,31] We checked for and removed outliers using an algorithm that identified very large increases or decreases between consecutive measurements and removed approximately 0.5% of observations as outliers. [29] Details of the outlier removal algorithm are given in the web appendix. In each superpixel and for each layer, we fit a Bayesian normal hierarchical random effects model with population and subject-specific random intercept and slope and a subject-specific residual variance using the JAGS package in R (*R2jags*). [32,33] Priors for each layer are provided in the web appendix.

For parameters that can be positive or negative, such as slopes or correlations, we calculated the posterior probability that the parameter was negative. If this probability is sufficiently high, or sufficiently low, it means the sign of the parameter is well determined by the data. For population parameters, we say that the parameter is *significant* if the posterior probability that the parameter is negative is either less than 0.025 (significantly positive) or greater than 0.975 (significantly negative). The Bayesian interpretation of *significant* is that the sign of the parameter (slope, correlation) is well determined, and that given the data and model, we are reasonably certain that the slope is less than zero (significantly negative) or greater than zero (significantly positive). This is a summary of the inference, not a test of a point null hypothesis. The Bayesian p-value can be interpreted as a classical one-sided p-value with the declaration of significance equivalent to using a two-sided classical p-value cutoff of 0.05. But this interpretation is secondary. Population parameters where significance is of interest include the population average slope and the correlation between the random intercepts and slopes. For patient-specific slopes, there is much less information about the magnitude of the slope as compared with the population slope and therefore, we used a less stringent criterion for declaring significance. We considered a slope in a given superpixel belonging to an individual patient as significantly negative if the posterior probability that the slope is negative was greater than 0.9. Conversely, if the posterior probability that the slope is negative was less than 0.1, we considered the lope in a given superpixel belonging to an individual patient as significantly positive. For each macular outcome measure and superpixel, we calculated the proportion of slopes that were significantly negative or significantly positive.

For each superpixel, we compared macular layers on the proportion of significantly negative slopes using a classical McNemar's test and plotted differences in proportions between layers in 36 heat maps and labeled each heat map cell with the two-sided p-value for the null hypothesis that the two proportions were equal. A Bonferroni adjustment for the 10 = (5 choose 2) tests within a superpixel would set alpha =0.005 and if the smallest p-value in a superpixel is less than 0.005 we can reject the null hypothesis that all layers have equal fractions of negative slopes in that superpixel at level alpha =0.05.

Definition of baseline glaucoma severity

We matched the macular superpixels to central 10-2 VF locations after taking into account the displacement of RGCs from the fovea as proposed by Drasdo et al. (Figure 2). [13,34,35] Figure 2 demonstrates that some superpixels have more than one matching VF location; in these cases, we exponentiated total deviation (TD) values at those locations, averaged and took a log to convert to the dB scale. Among the 36 superpixels, 4 superpixels

(superpixels 2.2, 2.7, 7.2 and 7.7, flagged with red asterisks on Figure 2) do not have any corresponding central VF locations; therefore, for this part of the analyses, we only included the remaining 32 superpixels with matching VF locations (TD values). We then divided individual superpixel-location pair combinations into those with mild to moderate (corresponding TD ≥−8 dB) and severe (corresponding TD <−8 dB) damage and calculated the proportion of superpixels with significant negative and positive slopes in the 2 severity groups for all macular outcomes of interest. This classification is based on our prior work showing that all macular structural measures reach or are close to their measurement floor when the corresponding functional damage at an individual location approaches −8 dB of sensitivity loss. [36]

Results

Table 1 summarizes the clinical and demographic characteristics of the study patients. The average (SD) age and baseline 10-2 visual field MD were 66.9 (8.5) years and −8.9 (5.9) dB. The average (SD) follow-up time was 3.60 (0.44) years and the average (SD) number of available OCT images was 7.3 (1.1). The number of outlying observations that were identified and removed out of 29,628 observations (i.e., superpixel thickness measurements) were 142 (0.48%) for FMT, 136 (0.46%) for ORL, 145 (0.49%) for GCC, 162 (0.55%) for GCIPL, and 145 (0.49%) for GCL. Empirical summary plots over time suggested that population and subject-specific profiles followed linear trends over time for all superpixels and macular measures.

Superpixels with the steepest negative average (population) slopes were mainly located within the superior and inferior paracentral and nasal (papillomacular bundle) regions for all macular measures except ORL (eFigure 1). Fastest ORL rates of change were seen mostly in peripheral nasal, inferior and temporal regions.

Correlations between estimated baseline thickness (superpixel intercepts) and slopes for inner macular measures were always significant when the correlation was less than (i.e., larger in magnitude) −0.26 for GCC, GCIPL and GCL; no such correlations were significant for ORL and only 1 of 36 were significant for FMT. The number of superpixels with significant correlations between random slopes and intercepts (estimated baseline thickness) was 20, 18, and 15 out of 36 superpixels for GCC, GCIPL and GCL, respectively. The range of the top 5 correlation coefficients were −0.43 to −0.50, −0.40 to −0.48 and −0.36 to −0.44 for GCC, GCIPL and GCL, respectively (eFigure 2).

For eyes and superpixels with corresponding TD measures, the average proportion of significant negative slopes or rates of change, a reflection of thinning of the macula, was 54.9%, 36.5%, 30.6%, 19.8% and 35.6% for FMT, GCC, GCIPL, GCL and ORL thickness measurements, respectively. Figure 3 shows a bar graph of all layers' proportion of significantly negative slopes (one sided Bayesian $p < 0.1$) for all 36 superpixels. Within the central superpixels 4.4, 4.5, 5.4, and 5.5, the proportion of worsening based on GCC thickness equaled or exceeded that of FMT. Table 2 provides the proportion of superpixels that were significantly negative or significantly positive among those that met the criteria for mild to moderate vs. severe damage based on the TD of the corresponding VF locations.

For GCC, GCIPL, and GCL, the proportion of significant negative slopes were overall lower at superpixels demonstrating severe functional damage compared to those with mild to moderate damage. In contrast, the proportion of significant negative slopes was similar for FMT in the two glaucoma severity groups. For ORL, the proportion of significant slopes was higher for superpixels with severe damage compared to those with mild to moderate damage. The proportion of significant negative slopes was higher for GCC compared to GCIPL and GCL in superpixels with either mild to moderate or severe damage.

eFigure 3 presents McNemar's test results comparing fraction of significant negative slopes for each pair of macular measures (FMT, ORL, GCC, GCIPL, and GCL thickness) within each of the 36 superpixels. As shown in this Figure, a higher proportion of significant negative GCC slopes compared to GCIPL slopes were identified in 10 out of 36 superpixels whereas in none GCIPL performed better than GCC. Similarly, this proportion was significantly higher for GCC slopes than GCL slopes in 33 out of 36 superpixels and GCL slopes were not superior to GCC slopes in any of the 36 superpixels. For most superpixels, FMT showed a higher proportion of negative slopes compared to other layers. However, in the paracentral superpixels (4.3, 4.4, 4.5, 4.6, 5.3, 5.4 and 5.5), FMT and GCC thickness had similar rates of significant negative slopes.

Figure 4 displays Venn diagrams of cross-classified counts of significant and nonsignificant negative slopes for FMT, GCC, and ORL thickness (Figure 4, left) and GCC, GCIPL, and GCL thickness (Figure 4, right). Significant negative FMT slopes were observed at 2,145 superpixels; among those 1,206 (56%) also had significant negative ORL slopes; In contrast, only 482 (35%) of the 1,376 significant GCC slopes also showed significant ORL slopes. Figure 4 right demonstrates that among 1677 superpixels demonstrating significantly negative slopes for any of the inner macular measures, 442 (26.4%), 139 (8.3%), and 79 (4.7%) showed worsening slopes only based on GCC, GCIPL, and GCL thickness, respectively. eFigure 4 displays Venn diagrams of cross-classified counts of significant and nonsignificant negative slopes for FMT, GCL, and ORL thickness (eFigure 4, left) and FMT, GCIPL, and ORL thickness (Figure 4, right).

eFigure 5 displays the magnitude of population slopes at each superpixel divided by (standardized) by their mean residual standard deviation as an indication of the signal to noise ratio for the various macular layers. At almost all superpixels, the signal to noise ratio was better for GCC thickness compared to GCIPL and GCL thickness. While the signal to noise ratio for FMT appear better than GCC in most superpixels, the FMT thickness measurements include ORL thickness values, which do not reflect damage from glaucoma.

The proportions of significant positive slopes were lower for FMT and ORL (1.8% and 1.4% overall, respectively) compared to inner macular layers (3.7-5.3%) and slightly increased with worse glaucoma severity for the inner macular measures (Table 2). Figure 5 presents a bar chart of the proportion of significant positive slopes for the five macular measures at each superpixel.

Discussion

We recently described a Bayesian hierarchical random intercept and slope (RIAS) model for estimating rates of change across the macular region. [29] This model more efficiently estimates individual and population rates of change compared to simple linear regression on data from one eye. We applied the model to five macular thickness measures for 3°×3° superpixels in individual eyes. The RIAS model estimates population means and population standard deviations of the baseline thickness and slopes (i.e., rates of change) and the correlation between superpixel-specific baseline thickness estimates (intercepts) and corresponding slopes. Additionally, the Bayesian paradigm can easily incorporate non-standard features in the data such as differing residual variances between subjects. [28] Further, Bayesian software has less difficulty with convergence in the presence of small sample sizes or when random effect variances are small. Bayesian models and hierarchical approaches have been used previously in some studies in the field of glaucoma, mostly focusing on functional aspects of glaucoma. [37–46]

We implemented this model to test the hypothesis that GCC thickness is the optimal macular measure for detecting change in eyes with moderate to advanced glaucoma; we compared the proportion of superpixels demonstrating significant worsening or improving slopes among five macular outcome measures. This is a topic of significant clinical interest as various OCT devices use different anatomical outcome measures to determine glaucomatous damage within the macular region. While none of the inner macular measures (GCC, GCIPL, or GCL) have been demonstrated to be superior in detection of early glaucoma, it is conceivable that these measures may not perform similarly for detection of glaucoma deterioration across the spectrum of glaucoma severity. [3,47–49] A major issue is that with advancing glaucoma damage, the task of segmentation of individual macular layers becomes more challenging; hence, measurements of thicker slabs of tissue such as GCC, the boundaries of which are easier to segment, may be less noisy. Another reason for potentially superior performance of GCC is that smaller amounts of positively correlated change within macular RNFL, GCL, and IPL are added and changes in the sum could be easier to detect than changes in the components. Most prior studies reported high reproducibility for global and sectoral macular thickness measurements. [50–52] Research from our laboratory has demonstrated intra- and inter-session variability to be very low at the superpixel level for all macular outcome measures and mostly uniform across the macular region. [30,53] This is another potential explanation for superior performance of the GCC in comparison to GCIPL and GCL as the measurement error compared to the magnitude of change is smaller with GCC. eFigure 5 confirms GCC's higher signal to noise ratio compared with GCIPL and GCL. Miraftabi et al. found that with advancing glaucoma and decreasing GCIPL and GCL thickness, measurement variability increased as the macular thickness approached its floor. [30]

Figures 3 and eFigure 3 show that although for the majority of superpixels FMT had a significantly higher proportion of significantly decreasing slopes compared to other layers, in the clinically important paracentral superpixels, the proportions were not different between FMT and GCC. The signal to noise ratio was better for GCC thickness across the macula compared to GCIPL and GCL thickness. Although the signal to noise ratio for FMT

appeared better than GCC in most superpixels, the FMT thickness measurements include ORL thickness values, which do not reflect damage from glaucoma.

We have previously demonstrated that, based on univariate regression analyses of thickness measurements at superpixels or superpixel clusters, GCC could be the best performing macular outcome for detection of glaucoma progression regardless of the disease stage.[15] However, that study used univariate regression analyses by subject to estimate rates of change within macular superpixels and clusters. Fitting univariate regression analyses to subjects separately is suboptimal statistically as population information from the entire cohort is ignored in estimating individual eye or superpixel intercepts and slopes. Within-superpixel correlations between repeated measures over time are ignored and population variance and estimation error are overestimated. The proposed Bayesian model addresses these shortcomings.

In this study, we designed rules for excluding outliers, reviewed longitudinal trends at the superpixel level, estimated the correlation between individual baseline thickness measurements and rates of change (slopes) and measured the proportion of superpixels with significant negative and positive slopes. The results confirm our prior findings and strongly suggest that GCC thickness seems to be the optimal macular outcome measure for monitoring eyes with moderate to advanced stages of glaucoma.

Population average rates of change (thinning) were fastest for FMT followed by GCC, GCIPL, and GCL as expected (eFigure 1). We compared the proportion of statistically significant negative and positive slopes at a Bayesian p-value of <0.1. Ganglion cell complex displayed more statistically significant progressive thinning among the inner macular measures. At the same time, the proportions of significant positive slopes were similar for all inner macular measures (3.9-5.3%, Table 2). Full macular thickness may demonstrate decreasing slope either due to decreasing GCC or ORL thickness or both. It is generally believed that ORL thinning is not caused by glaucoma and that the observed changes might be partially related to aging. [16–18] Unpublished analyses on longitudinal structural-function relationships from our previously published manuscript also confirm this.[13] We demonstrated, in that manuscript, that the rates of change of the 10-2 VF total deviation values at individual test locations were significantly correlated to GCC, GCIPL, GCL, and FMT thickness changes at corresponding superpixels in that order. The same analyses showed that changes in ORL thickness over time at the level of superpixels did not display any correlations ($r = -0.05$; $p = 0.595$) to changes in the total deviation values at corresponding test locations. Thus, we believe that GCC is preferable as a measure of functional decline in glaucoma. Interestingly, the proportion of significant GCC negative slopes was equal to or higher than that in FMT in some paracentral superpixels suggesting that most of the FMT change observed in those superpixels occurred in the inner retina. We performed pairwise comparison of the proportion of significantly negative slopes for all macular measures (eFigure 3). A higher proportion of significant negative GCC slopes were detected in 10 out of 36 superpixels compared with GCIPL and in 33 out of 36 superpixels compared to GCL.

One of the main aims of the current study was to assess the comparative performance of the macular measures as a function of glaucomatous damage in superpixels. We defined glaucomatous damage by the magnitude of the TD at test locations corresponding to the macular superpixels and set a cutoff point of −8 dB specifically chosen based on our prior findings that macular measures reached their measurement floor at superpixel level at approximately this level of functional loss. [36] Our results confirmed two findings: first, all inner macular measures demonstrate a reduction in the proportion of significant negative slopes detected over time in eyes with worse glaucoma damage (i.e., TD <−8 dB) compared to those with less severe damage. Second, GCC measurements are best able to identify decreasing slopes compared to GCIPL and GCL regardless of the level of glaucoma damage. The proportion of positive slopes only slightly increased with worsening glaucoma for all the 3 inner macular measures. Although it is commonly assumed that positive slopes represent mostly noise, we plan to explore this issue in more detail when this cohort reaches a longer follow-up time. The differences among inner retinal layers with regard to detection rates of negative slopes are clinically relevant. In the group with mild to moderate visual field damage, GCC detected 7% more worsening superpixels compared to GCIPL and about 18% more deteriorating superpixels than GCL (Table 2). This would translate to about 2.5 to 6.5 more superpixels, on average, being detected as deteriorating by GCC slopes (compared to GCIPL and GCL slopes, respectively); given the large size of superpixels in this study (3×3 degrees or roughly 1×1mm), these would translate to large areas of the macula where additional evidence of change could be identified. The corresponding numbers for the severe glaucoma group were 1.5 and 4.5 more superpixels detected by GCC slopes compared to GCIPL and GCL slopes. As FMT is a combination of the ORL and GCC, it would be expected to show a significant decrease in thickness when either of its components is progressively thinning. In contrast, ORL and GCC slopes were less likely to be simultaneously decreasing as compared to either one with FMT (Figure 4, left). This supports our conclusion that although a higher proportion of significantly decreasing superpixels were observed with FMT, GCC thickness contains the more clinically relevant information for detection of structural change in the macular region. The stronger structure-function relationships observed with GCC compared to FMT in our prior study supports this conclusion. [13] The second Venn diagram on Figure 4 (on the right) also demonstrates that GCC slopes were more likely to detect a significant thinning of the inner macula compared to GCIPL or GCL slopes.

Our results provide strong evidence that GCC thickness is potentially the best structural outcome measure for monitoring and detecting change over time in the macular region in eyes with moderate to severe glaucoma with the current OCT technology. Our conclusions are based on the following premises: 1) GCC thickness was able to detect the highest proportion of significantly negative rates of change, i.e., worsening, among the inner macular measures; 2) the location of the deteriorating superpixels matched the region where disease worsening is expected to occur in a group of eyes with moderate to advanced glaucoma; 3) superpixels demonstrating significantly negative GCC rates of change, were less likely to show significant thinning of the ORL thickness or outer retina compared to those demonstrating significant FMT change; outer retinal changes are widely believed not to be related to glaucomatous damage; 3) although the proportion of significant negative

rates of change (slopes) decreased in the superpixels with severe functional damage, GCC thickness was still more likely to detect change over time in this group; 4) a large amount of FMT change correlated with changes in the ORL thickness and hence, was influenced by nonglaucomatous changes in outer retinal layers. These findings along with the stronger longitudinal structural-functional correlations seen between GCC rates of change and functional rates of change in comparison to FMT and the patterns of ongoing damage in the macular region strongly point to the GCC thickness being the optimal structural measure for detection of change in moderate to advanced glaucoma.

All OCT devices are able to estimate and provide GCC thickness measurements with only minimal software modifications by the manufacturers and we strongly recommend that GCC thickness measurements be made available for detection of disease progression on all OCT platforms. The addition of GCC measurements to the current algorithms for detection of change would facilitate and optimize detection of structural deterioration in glaucoma eyes. Correct estimation of local slopes and the uncertainty in their estimates across the macular region where there are strong spatial correlations is the subject of our ongoing work. Given the evidence provided in this manuscript, it is expected that even with the preliminary available univariate approaches and algorithms provided by some of the current OCT proprietary software, the detection of change would become more efficient using GCC thickness as the outcome measure of choice. Our future studies will focus on how best to summarize the regional and global rates of change, explore prediction of functional change with longer follow-up time, and provide better data visualization with regard to detection of progression in real-time.

Supplementary Material

Refer to Web version on PubMed Central for supplementary material.

Acknowledgement

This work was supported by an NIH R01 grant (R01-EY029792), an unrestricted Departmental Grant from Research to Prevent Blindness, and an unrestricted grant from Heidelberg Engineering.

References

1. Mohammadzadeh V, Fatehi N, Yarmohammadi A, et al. Macular Imaging with Optical Coherence Tomography in Glaucoma. Surv Ophthalmol. 2020 Mar 19.
2. Lee KS, Lee JR, Na JH, Kook MS. Usefulness of macular thickness derived from spectral-domain optical coherence tomography in the detection of glaucoma progression. Invest Ophthalmol Vis Sci. 2013;54(3):1941–1949. [PubMed: 23422822]
3. Chien JL, Ghassibi MP, Patthanathamrongkasem T, et al. Glaucoma Diagnostic Capability of Global and Regional Measurements of Isolated Ganglion Cell Layer and Inner Plexiform Layer. J Glaucoma. 2017;26(3):208–215. [PubMed: 27811573]
4. Martucci A, Toschi N, Cesareo M, et al. Spectral Domain Optical Coherence Tomography Assessment of Macular and Optic Nerve Alterations in Patients with Glaucoma and Correlation with Visual Field Index. J Ophthalmol. 2018;2018:6581846. [PubMed: 30402278]
5. Hood DC, Raza AS, de Moraes CG, Liebmann JM, Ritch R. Glaucomatous damage of the macula. Prog Retin Eye Res. 2013;32:1–21. [PubMed: 22995953]

6. Hood DC. Improving our understanding, and detection, of glaucomatous damage: An approach based upon optical coherence tomography (OCT). Prog Retin Eye Res. 2017;57:46–75. [PubMed: 28012881]
7. Sung KR, Sun JH, Na JH, Lee JY, Lee Y. Progression detection capability of macular thickness in advanced glaucomatous eyes. Ophthalmology. 2012;119(2):308–313. [PubMed: 22182800]
8. Wong JJ, Chen TC, Shen LQ, Pasquale LR. Macular imaging for glaucoma using spectral-domain optical coherence tomography: a review. Semin Ophthalmol. 2012;27(5-6):160–166. [PubMed: 23163271]
9. Bowd C, Zangwill LM, Weinreb RN, Medeiros FA, Belghith A. Estimating Optical Coherence Tomography Structural Measurement Floors to Improve Detection of Progression in Advanced Glaucoma. Am J Ophthalmol. 2017;175:37–44. [PubMed: 27914978]
10. Na JH, Sung KR, Baek S, et al. Detection of glaucoma progression by assessment of segmented macular thickness data obtained using spectral domain optical coherence tomography. Invest Ophthalmol Vis Sci. 2012;53(7):3817–3826. [PubMed: 22562510]
11. Tatham AJ, Medeiros FA. Detecting Structural Progression in Glaucoma with Optical Coherence Tomography. Ophthalmology. 2017;124(12S):S57–S65. [PubMed: 29157363]
12. Nguyen AT, Greenfield DS, Bhakta AS, Lee J, Feuer WJ. Detecting Glaucoma Progression Using Guided Progression Analysis with OCT and Visual Field Assessment in Eyes Classified by International Classification of Disease Severity Codes. Ophthalmology Glaucoma. 2019;2(1):36–46. [PubMed: 32672556]
13. Mohammadzadeh V, Rabiolo A, Fu Q, et al. Longitudinal Macular Structure-Function Relationships in Glaucoma. Ophthalmology. 2020 Jul 1;127(7):888–900. [PubMed: 32173112]
14. Harwerth RS, Carter-Dawson L, Shen F, Smith EL, 3rd, Crawford ML. Ganglion cell losses underlying visual field defects from experimental glaucoma. Invest Ophthalmol Vis Sci. 1999;40(10):2242–2250. [PubMed: 10476789]
15. Rabiolo A, Mohammadzadeh V, Fatehi N, et al. Comparison of Rates of Progression of Macular OCT Measures in Glaucoma. Transl Vis Sci Technol. 2020(In Press.).
16. Vianna JR, Butty Z, Torres LA, et al. Outer retinal layer thickness in patients with glaucoma with horizontal hemifield visual field defects. Br J Ophthalmol. 2018.
17. Xu Q, Li Y, Cheng Y, Qu Y. Assessment of the effect of age on macular layer thickness in a healthy Chinese cohort using spectral-domain optical coherence tomography. BMC Ophthalmol. 2018;18(1):169. [PubMed: 29996804]
18. Nieves-Moreno M, Martínez-de-la-Casa JM, Morales-Fernández L, Sánchez-Jean R, Sáenz-Francés F, García-Feijoó J. Impacts of age and sex on retinal layer thicknesses measured by spectral domain optical coherence tomography with Spectralis. PLoS One. 2018;13(3):e0194169. [PubMed: 29522565]
19. Jammal AA, Thompson AC, Mariottoni EB, et al. Rates of Glaucomatous Structural and Functional Change from a Large Clinical Population: The Duke Glaucoma Registry Study. Am J Ophthalmol. 2020.
20. Chua J, Kadziauskiene A, Wong D, et al. One year structural and functional glaucoma progression after trabeculectomy. Sci Rep. 2020;10(1):2808. [PubMed: 32071369]
21. Wu Z, Crabb DP, Chauhan BC, Crowston JG, Medeiros FA. Improving the Feasibility of Glaucoma Clinical Trials Using Trend-Based Visual Field Progression End Points. Ophthalmology Glaucoma. 2019;2(2):72–77. [PubMed: 32632403]
22. Liebmann K, De Moraes CG, Liebmann JM. Measuring Rates of Visual Field Progression in Linear Versus Nonlinear Scales: Implications for Understanding the Relationship Between Baseline Damage and Target Rates of Glaucoma Progression. J Glaucoma. 2017;26(8):721–725. [PubMed: 28692594]
23. Zhang C, Tatham AJ, Abe RY, et al. Corneal Hysteresis and Progressive Retinal Nerve Fiber Layer Loss in Glaucoma. Am J Ophthalmol. 2016;166:29–36. [PubMed: 26949135]
24. Ariyo O, Lesaffre E, Verbeke G, Quintero A. Model selection for Bayesian linear mixed models with longitudinal data: Sensitivity to the choice of priors. Communications in Statistics - Simulation and Computation. 2019:1–25.

25. Bryan SR, Eilers PHC, Rosmalen JV, et al. Bayesian hierarchical modeling of longitudinal glaucomatous visual fields using a two-stage approach. Stat Med. 2017;36(11):1735–1753. [PubMed: 28152571]
26. Weiss RE. Bayesian methods for data analysis. Am J Ophthalmol. 2010;149(2):187–188 e181. [PubMed: 20103051]
27. Fitzmaurice GM, Laird NM, Ware JH. Applied longitudinal analysis. John Wiley & Sons. 2012 Oct 23.
28. Harville D Extension of the Gauss-Markov theorem to include the estimation of random effects. The Annals of Statistics. 1976 Mar 1:384–95.
29. Mohammadzadeh V, Su E, Heydar Zadeh S, et al. Estimating Ganglion Cell Complex Rates of Change With Bayesian Hierarchical Models. Transl Vis Sci Technol. 2021;10(4).
30. Miraftabi A, Amini N, Gornbein J, et al. Local Variability of Macular Thickness Measurements With SD-OCT and Influencing Factors. Transl Vis Sci Technol. 2016;5(4):5.
31. Weiss RE. Modeling longitudinal data. Springer Science & Business Media. 2005 Jun 28.
32. Denwood MJ. runjags: An R package providing interface utilities, model templates, parallel computing methods and additional distributions for MCMC models in JAGS. Journal of Statistical Software. 2016 Jul 26;71(9):1–25.
33. Team RC. R: A language and environment for statistical computing. R Foundation for Statistical Computing, Vienna, Austria 2013.
34. Drasdo N, Millican CL, Katholi CR, Curcio CA. The length of Henle fibers in the human retina and a model of ganglion receptive field density in the visual field. Vision Res. 2007;47(22):2901–2911. [PubMed: 17320143]
35. Raza AS, Cho J, de Moraes CG, et al. Retinal ganglion cell layer thickness and local visual field sensitivity in glaucoma. Arch Ophthalmol. 2011;129(12):1529–1536. [PubMed: 22159673]
36. Miraftabi A, Amini N, Morales E, et al. Macular SD-OCT Outcome Measures: Comparison of Local Structure-Function Relationships and Dynamic Range. Invest Ophthalmol Vis Sci. 2016;57(11):4815–4823. [PubMed: 27623336]
37. Bae HW, Rho S, Lee HS, et al. Hierarchical cluster analysis of progression patterns in open-angle glaucoma patients with medical treatment. Invest Ophthalmol Vis Sci. 2014;55(5):3231–3236. [PubMed: 24781944]
38. Murata H, Zangwill LM, Fujino Y, et al. Validating Variational Bayes Linear Regression Method With Multi-Central Datasets. Invest Ophthalmol Vis Sci. 2018;59(5):1897–1904. [PubMed: 29677350]
39. Anderson AJ. Estimating the true distribution of visual field progression rates in glaucoma. Invest Ophthalmol Vis Sci. 2015;56(3):1603–1608. [PubMed: 25678691]
40. Murata H, Araie M, Asaoka R. A new approach to measure visual field progression in glaucoma patients using variational bayes linear regression. Invest Ophthalmol Vis Sci. 2014;55(12):8386–8392. [PubMed: 25414192]
41. Anderson AJ, Johnson CA. How useful is population data for informing visual field progression rate estimation? Invest Ophthalmol Vis Sci. 2013;54(3):2198–2206. [PubMed: 23462750]
42. Russell RA, Malik R, Chauhan BC, Crabb DP, Garway-Heath DF. Improved estimates of visual field progression using bayesian linear regression to integrate structural information in patients with ocular hypertension. Invest Ophthalmol Vis Sci. 2012;53(6):2760–2769. [PubMed: 22467579]
43. Medeiros FA, Zangwill LM, Weinreb RN. Improved prediction of rates of visual field loss in glaucoma using empirical Bayes estimates of slopes of change. J Glaucoma. 2012;21(3):147–154. [PubMed: 21423039]
44. Medeiros FA, Zangwill LM, Mansouri K, Lisboa R, Tafreshi A, Weinreb RN. Incorporating risk factors to improve the assessment of rates of glaucomatous progression. Invest Ophthalmol Vis Sci. 2012;53(4):2199–2207. [PubMed: 22410555]
45. Medeiros FA, Zangwill LM, Girkin CA, Liebmann JM, Weinreb RN. Combining structural and functional measurements to improve estimates of rates of glaucomatous progression. Am J Ophthalmol. 2012;153(6):1197–1205 e1191. [PubMed: 22317914]

46. Medeiros FA, Leite MT, Zangwill LM, Weinreb RN. Combining structural and functional measurements to improve detection of glaucoma progression using Bayesian hierarchical models. Invest Ophthalmol Vis Sci. 2011;52(8):5794–5803. [PubMed: 21693614]

47. Pazos M, Dyrda AA, Biarnes M, et al. Diagnostic Accuracy of Spectralis SD OCT Automated Macular Layers Segmentation to Discriminate Normal from Early Glaucomatous Eyes. Ophthalmology. 2017;124(8):1218–1228. [PubMed: 28461015]

48. Kim HJ, Lee SY, Park KH, Kim DM, Jeoung JW. Glaucoma Diagnostic Ability of Layer-by-Layer Segmented Ganglion Cell Complex by Spectral-Domain Optical Coherence Tomography. Invest Ophthalmol Vis Sci. 2016;57(11):4799–4805. [PubMed: 27654408]

49. Chua J, Tan B, Ke M, et al. Diagnostic Ability of Individual Macular Layers by Spectral-Domain OCT in Different Stages of Glaucoma. Ophthalmol Glaucoma. 2020;3(5):314–326. [PubMed: 32980035]

50. Francoz M, Fenolland JR, Giraud JM, et al. Reproducibility of macular ganglion cell-inner plexiform layer thickness measurement with cirrus HD-OCT in normal, hypertensive and glaucomatous eyes. Br J Ophthalmol. 2014;98(3):322–328. [PubMed: 24307717]

51. Lee MW, Park KS, Lim HB, Jo YJ, Kim JY. Long-term reproducibility of GC-IPL thickness measurements using spectral domain optical coherence tomography in eyes with high myopia. Sci Rep. 2018;8(1):11037. [PubMed: 30038425]

52. Kim KE, Yoo BW, Jeoung JW, Park KH. Long-Term Reproducibility of Macular Ganglion Cell Analysis in Clinically Stable Glaucoma Patients. Invest Ophthalmol Vis Sci. 2015;56(8):4857–4864. [PubMed: 25829417]

53. Nouri-Mahdavi K, Fatehi N, Caprioli J. Longitudinal Macular Structure-Function Relationships in Glaucoma and Their Sources of Variability. Am J Ophthalmol. 2019;207:18–36. [PubMed: 31078529]

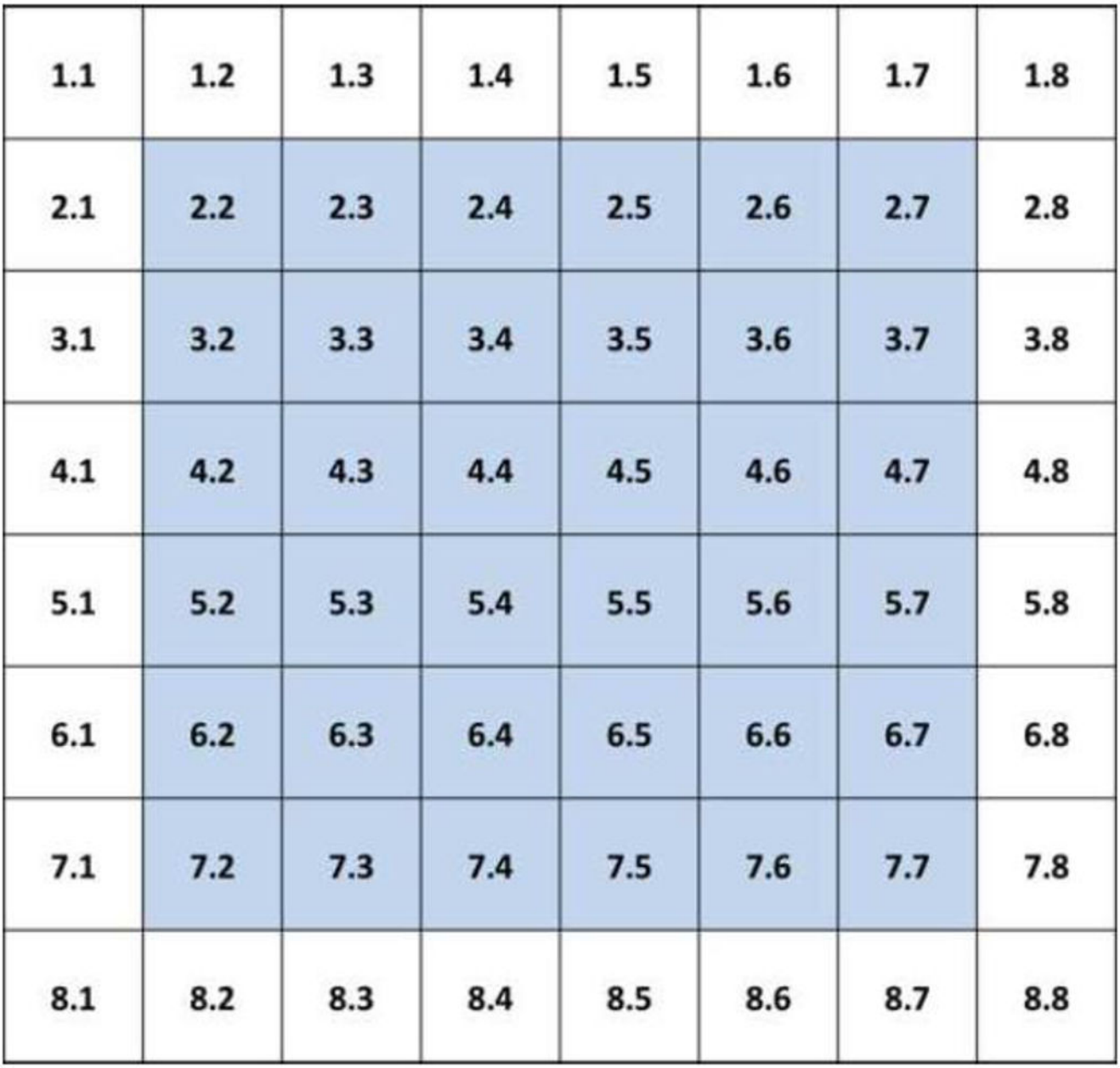

Figure 1.

The Posterior Pole Algorithm of the Spectralis (Heidelberg Engineering, Heidelberg, Germany) spectral domain OCT provides an 8×8 array of 3°×3°superpixels within the central 24° of the macula. Due to high variability observed in the outer superpixels, we included only the central 36 superpixels (colored in blue) for this study.

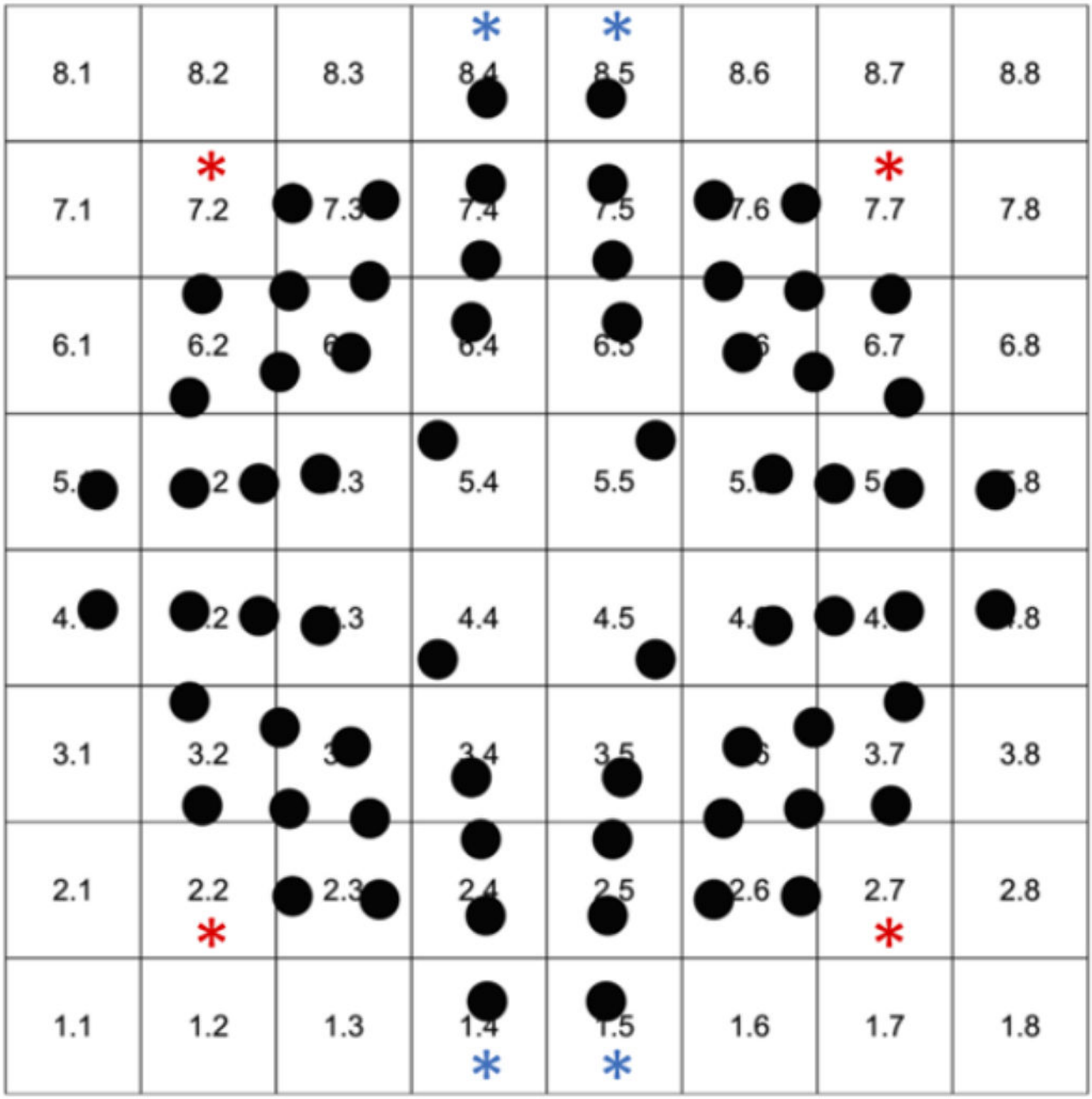

Figure 2.

An overlay of 10-2 visual field (VF) locations on the 8×8 array of macular superpixels. Of the 36 superpixels included in this analysis, only 32 superpixels have corresponding TD measures and superpixels 2.2, 2.7, 7.2 and 7.7 were excluded from analyses related to the influence of glaucoma severity. (with permission from Mohammadzadeh et al. Ophthalmology. 2020 [13]).

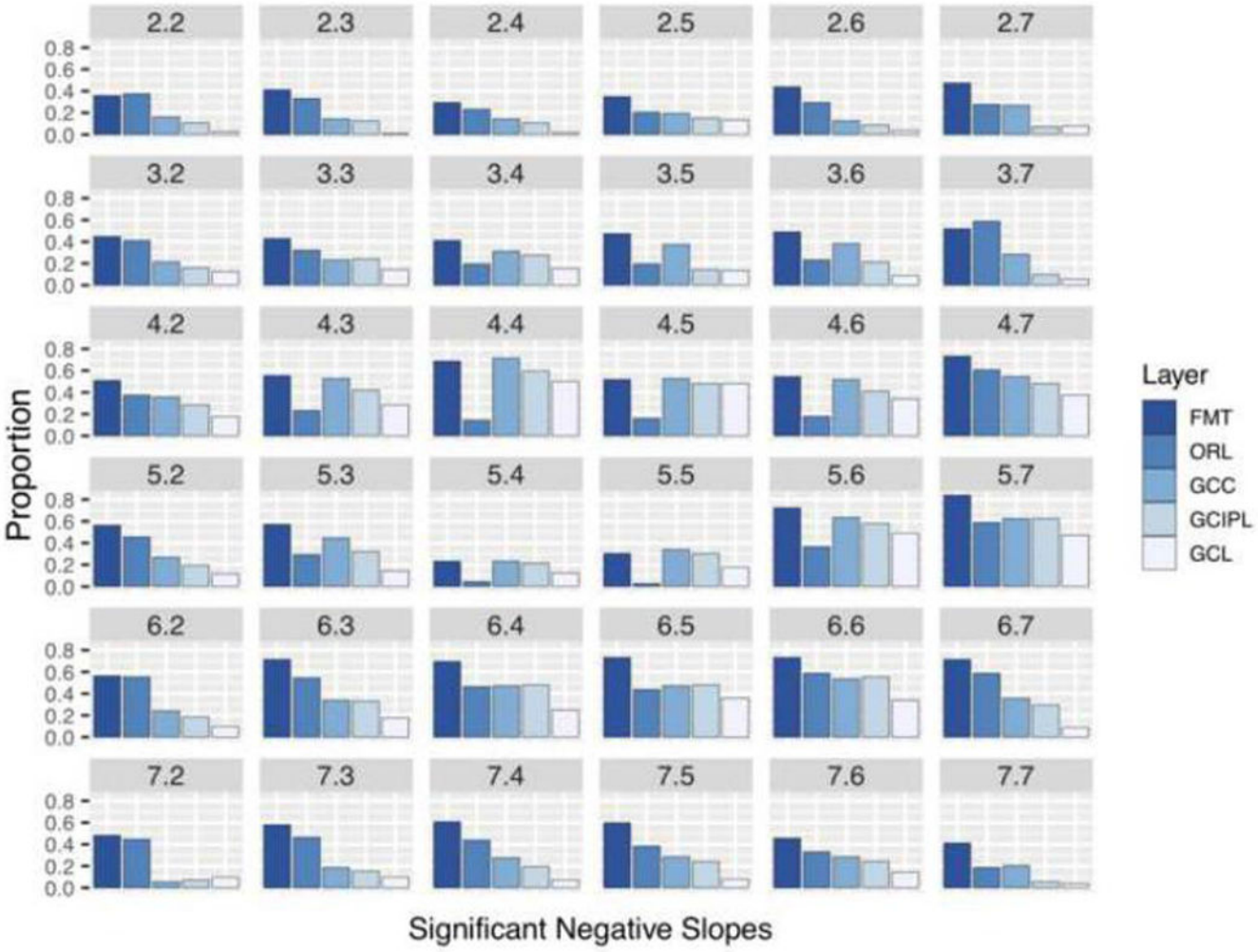

Figure 3.

For each superpixel, a bar chart of the proportion of study eyes with significant negative slopes ($p < 0.1$) for each macular outcome measure. FMT, full macular thickness; ORL, outer retinal layers, GCC, ganglion cell complex; GCIPL, ganglion cell/inner plexiform layer; GCL, ganglion cell layer.

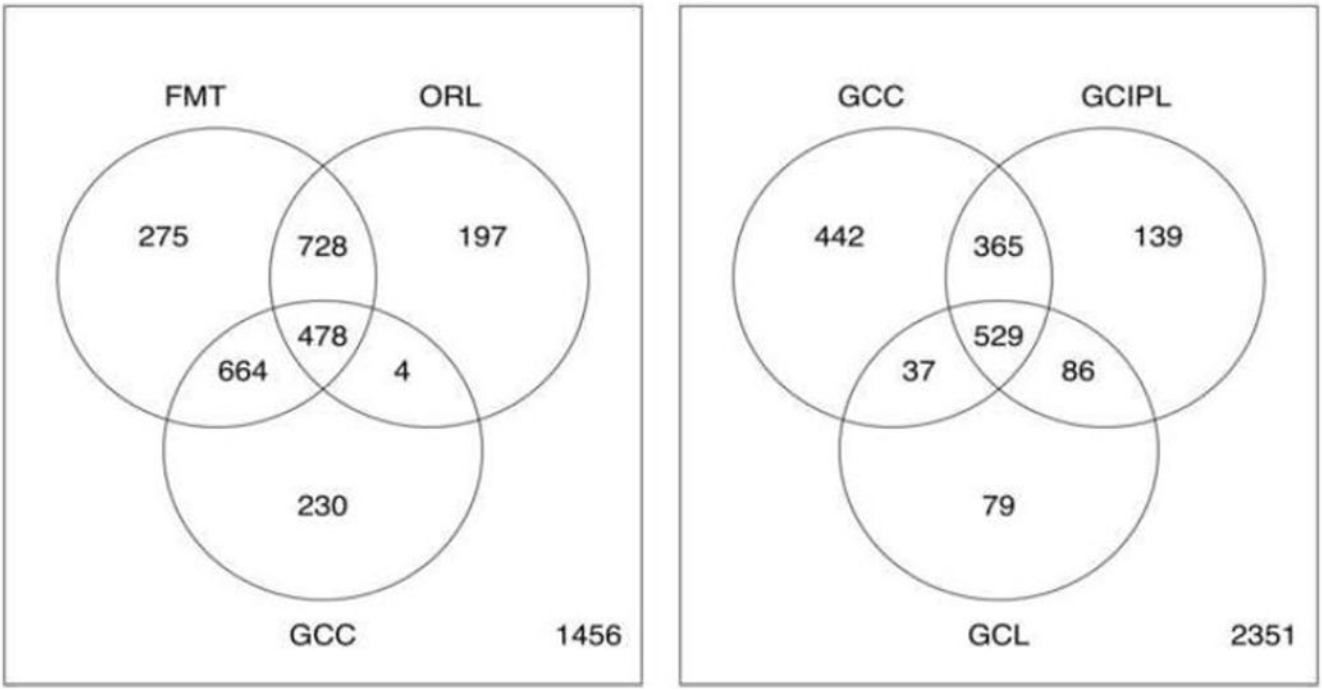

Figure 4.

(Left) Venn diagram displays the number of superpixel combinations for full macular thickness (FMT), outer retinal layer (ORL) thickness, and ganglion cell complex (GCC) thickness based on whether their slopes were significantly negative ($p < 0.1$) or not. For 1456 superpixels, the p-values for all three slopes were >0.1. (Right) Venn diagram displays the number of progressing and stable superpixel combinations for GCC, GCIPL (ganglion cell/inner plexiform layer), and ganglion cell layer (GCL) thickness measures.

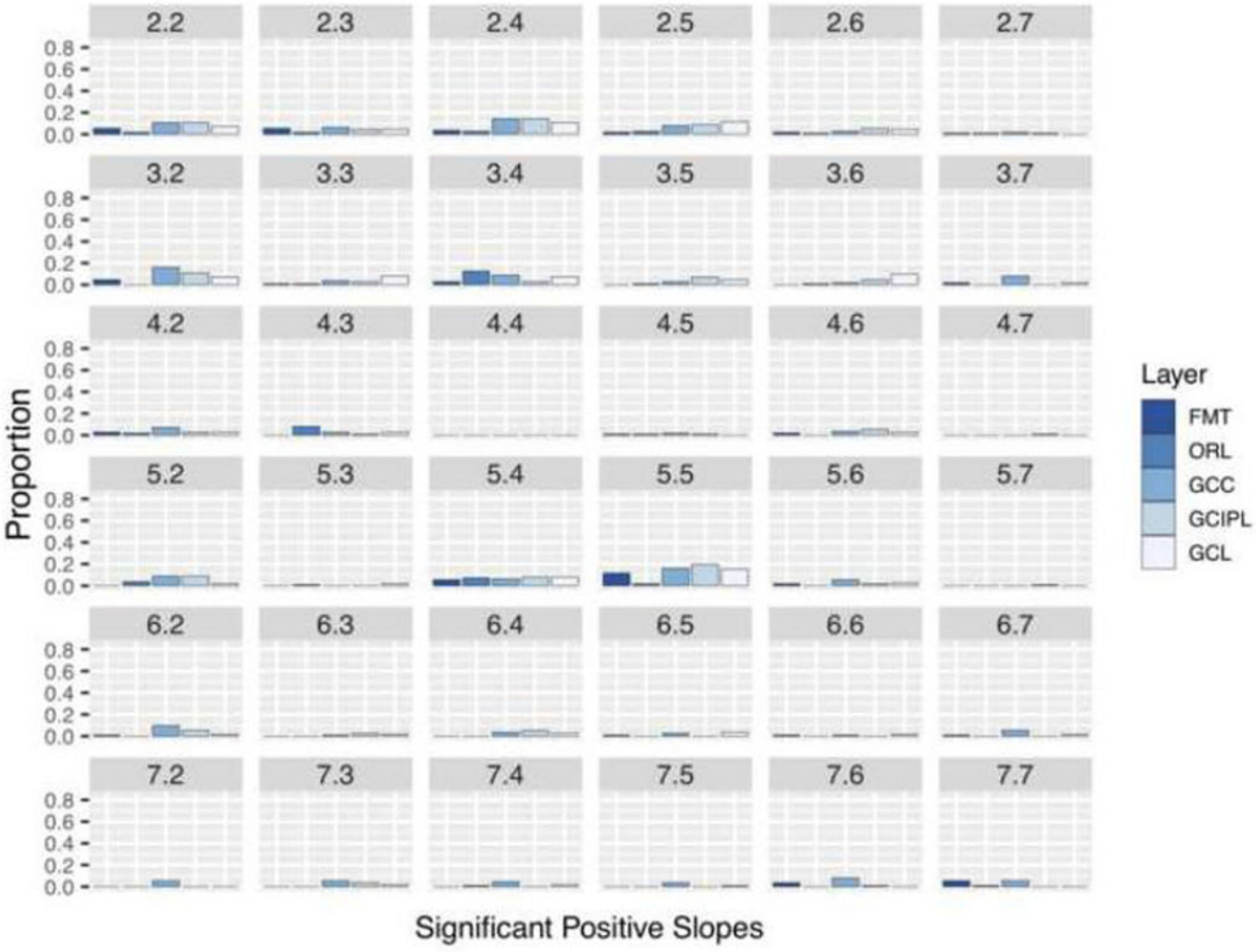

Figure 5.

For each superpixel, a bar chart of the proportion of study eyes with significant positive slopes ($p < 0.1$) for each layer. FMT, full macular thickness; ORL, outer retinal layers, GCC, ganglion cell complex; GCIPL, ganglion cell/inner plexiform layer; GCL, ganglion cell layer.

Table 1.

Demographic and clinical characteristics of the study eyes.

Age (years)	
Mean (SD)	66.9 (8.5)
Range	39.7 to 81.2
Gender (%)	
Female	70 (62.5%)
Male	42 (37.5%)
Ethnicity (%)	
Caucasian	59 (52.7%)
Asian	24 (21.4%)
African American	15 (13.4%)
Hispanic	14 (12.5%)
Baseline 10-2 MD (dB)	
Median (IQR)	−7.7 (−11.9 to −4.2)
Mean (SD)	−8.9 (5.9)
Range	−25.1 to −0.4
Baseline 24-2 MD (dB)	
Median (IQR)	−6.8 (−12.2 to −4.3)
Mean (SD)	−8.7 (6.1)
Range	−26.4 to −0.3
Follow up (years)	
Mean (SD)	3.60 (0.44)
Range	1.94 to 4.20
Signal Strength	
Mean (SD)	27.8 (3.1)
Range	21 to 36
Baseline FMT (μm)	
Mean (SD)	279.2 (30.8)
Range	211 to 379
Baseline ORL (μm)	
Mean (SD)	202.2 (19.8)
Range	147 to 262
Baseline GCC (μm)	
Mean (SD)	77.0 (20.2)
Range	37 to 154
Baseline GCIPL (μm)	
Mean (SD)	51.8 (14.4)
Range	26 to 112

Baseline GCL (μm)	
Mean (SD)	26.6 (9.0)
Range	9 to 64

MD = mean deviation; SD = standard deviation; FMT= full macular thickness; ORL= outer retina layer; GCC= ganglion cell complex; GCIPL= ganglion cell/inner plexiform layer; GCL ganglion cell layer

Table 2.

Proportion of significant negative and positive slopes (defined as Bayesian p value <0.1) for study eyes with corresponding TD and by glaucoma severity. Mild to moderate glaucoma damage at a given superpixel is defined as total deviation (TD) ≥−8 dB in the corresponding 10-2 visual field location and severe damage is defined as TD <−8 dB. FMT = full macular thickness; ORL = outer retinal layers; GCC = ganglion cell complex; GCIPL = ganglion cell/inner plexiform layer; GCL = ganglion cell layer.

	Significant Negative Slopes			Significant Positive Slopes		
Layer	**All**	**Mild to Moderate**	**Severe**	**All**	**Mild to Moderate**	**Severe**
FMT	1932/3519 (54.9%)	1387/2534 (54.7%)	545/985 (55.3%)	58/3519 (1.6%)	53/2534 (2.1%)	5/985 (0.5%)
ORL	1254/3519 (35.6%)	806/2534 (31.8%)	448/985 (45.5%)	54/3519 (1.5%)	49/2534 (1.9%)	5/985 (0.5%)
GCC	1286/3519 (36.5%)	1063/2534 (41.9%)	223/985 (22.6%)	186/3519 (5.3%)	110/2534 (4.3%)	76/985 (7.7%)
GCIPL	1075/3518 (30.6%)	892/2533 (35.2%)	183/985 (18.6%)	142/3518 (4.0%)	91/2533 (3.6%)	51/985 (5.2%)
GCL	698/3518 (19.8%)	592/2533 (23.4%)	106/985 (10.8%)	138/3518 (3.9%)	93/2533 (3.7%)	45/985 (4.6%)